http://www.ejchem.net

ISSN: 0973-4945; CODEN ECJHAO
E-Journal of Chemistry
2012, **9(4)**, 2191-2204

Structural and Theoretical Studies of 2-amino-3-nitropyridine

N. S. AL-HOKBANY[a], A. A. DAHY[b], I. KH.WARAD[a] , N. M. ABD EL-SALAM[c], S. T. AKRICHE[d], M. RZAIGUI[d], U. KARAMA[a], AND R. M. MAHFOUZ[a*]

[a]Chemistry Department, Faculty of Science, King Saud University, P.O. Box 2455, Riyadh 11451, Saudi Arabia
[b]Chemistry Department, Faculty of Science, Assiut Uniersity, Assiut 71516, Egypt
[c]Natural Sciences Department, Riyadh Community College, King Saud University, P.O. Box 28095, Riyadh 11437, Saudi Arabia
[d]Laboratoire de Chimie des Matériaux, Faculté des Sciences de Bizerte, 7021 Zarzouna Bizerte, Tunisia
rmhfouz@ksu.edu.sa

Received 02 November 2011; Accepted 07 January 2012

Abstract: Geometrical optimization, spectroscopic analysis, electronic structure and nuclear magnetic resonance of 2-amino-3-nitropyridine (ANP) were investigated by utilizing *ab-initio* (MP2) and DFT(B3LYP) using 6-311++G(d,p) basis set. Geometrical parameters (bond lengths, bond angles and torsion angles) were computed and compared with the experimental values obtained using X-ray single crystal measurements of the title compound. IR spectra were obtained and assigned by vibrational analysis. Comparing the theoretically calculated values (bond lengths, bond and dihedral angles) using both B3LYP/6-311++G(d,p) and MP2/6-311++G(d,p) methods of calculations with the experimentally determined data by X-ray single crystal measurements, all the data obtained in this investigation were considered to be reliable. The theoretical infrared spectra have been successfully simulated by means of DFT and MP2 levels of calculations. The ^{1}H and ^{13}C nuclear magnetic resonance (NMR) chemical shifts of 2-amino-3-nitropyridine were calculated using the GIAO method in DMSO solution using IEF-PCM model and compared with the experimental data. Intramolecular hydrogen bonding interaction in this compound was investigated by means of the NBO analysis. The calculated HOMO and LUMO energies show that charge transfer occurs within the molecule.

Key words: 2-amino-3-nitropyridine; geometrical optimization; vibrational analysis; NBO analysis.

Introduction

Crystal structures and spectroscopic properties of conjugated systems have been a subject of immense interest due to the possibility of using these systems as non-linear optical (NLO) materials.[1-3] A common and often productive route to such materials has been to utilize molecules with electron donating and accepting moieties attached to a conjugated system. Aromatic amino-nitro systems are potentially useful NLO materials and typically cations derived from such molecules have been used within hydrogen bonded organic anionic network, or as counter ions in organic/inorganic salts.[4-7]

Crystal structure of 2-amino-3-nitropyridine has been reported.[8] The vibrational spectra of substituted pyridine have been extensively investigated.[9] Recently ab-initio Hartree-Fock and DFT study on vibrational spectra and molecular structures of 2-amino-3,4-, and 5-nitropyridine have been published.[10]

In the present investigation detailed quantum chemical calculations including geometrical optimization, vibrational spectra, NMR chemical shifts and electronic transition were performed using density functional theory calculations. The theoretically calculated values were evaluated and compared with the available experimental data of this compound.

Computational Details

The molecular geometry optimization, energy and vibrational frequency calculations were performed with the GAUSSIAN 03W software package[11], using DFT(B3LYP) and MP2 levels combined with the standard 6-311++G(d,p) basis set. Using triple zeta basis set for valence electrons with polarization and diffusion function for both heavy atoms and hydrogen is reliable. The Cartesian representation of the theoretical force constants were computed at the optimized geometry by assuming C_s point group symmetry. Scaling of the force field was performed using 0.9613 and 0.942 scale factors for B3LYP and MP2 levels of calculations, respectively. The geometry was fully optimized without any constraint with the help of analytical gradient procedure. The optimized structure is a minimum because all the frequencies are positive. By the use of GAUSSVIEW molecular visualization program[12] with symmetry considerations along with available related molecules, vibrational wavenumber assignments were made with a high degree of accuracy.

The natural bonding orbital (NBO) calculations were performed at the B3LYP/6-31G++(d,p) method in order to investigate the electronic structures of the optimized geometry corresponding to the formation of C– H---O and C– H---N hydrogen bonding. The hyperconjugative interaction energy was deduced from the second- order perturbation approach.[13]

$$E^{(2)} = \Delta E_{ij} = q_i \frac{F_{(ij)}^2}{\varepsilon_j - \varepsilon_i},$$

where q_i, is the donor orbitals occupancy, ε_j, ε_i the diagonal elements (orbital energies) and $F_{(i,j)}$ is the off diagonal NBO Fock matrix elements. These calculations are valuable to

gain insight into the vibrational spectroscopy, molecular parameters, NMR chemical shifts and electronic transitions of the title structure. All the calculations are performed by using the Gaussian 03W program package on a personal computer.[11]

Results and Discussion

Geometrical parameters

The labeling of atoms in 2-amino-3-nitropyridine is given in Figure 1. The calculated structural parameters, total energy and dipole moment using B3LYP and MP2 methods are collected in Table 1. The bond lengths and angles determined at the DFT level of theory are in good agreement with the X-ray data.[8] From the theoretical values we can find that most of the optimized bond lengths are slightly longer or shorter than the experimental values at the MP2 and DFT levels, due to the fact that the theoretical calculations belong to isolated molecules in gaseous phase and the experimental results belong to molecule in solid state. The results of dihedral calculations indicate that the NH_2 and NO_2 groups are coplanar with pyridine ring as was demonstrated by X-ray diffraction measurements. Comparing bond angles and lengths of B3LYP with those of MP2, as a whole the formers in majority case are bigger than the latter and the B3LYP calculated values correlates well compared with the experimental results.

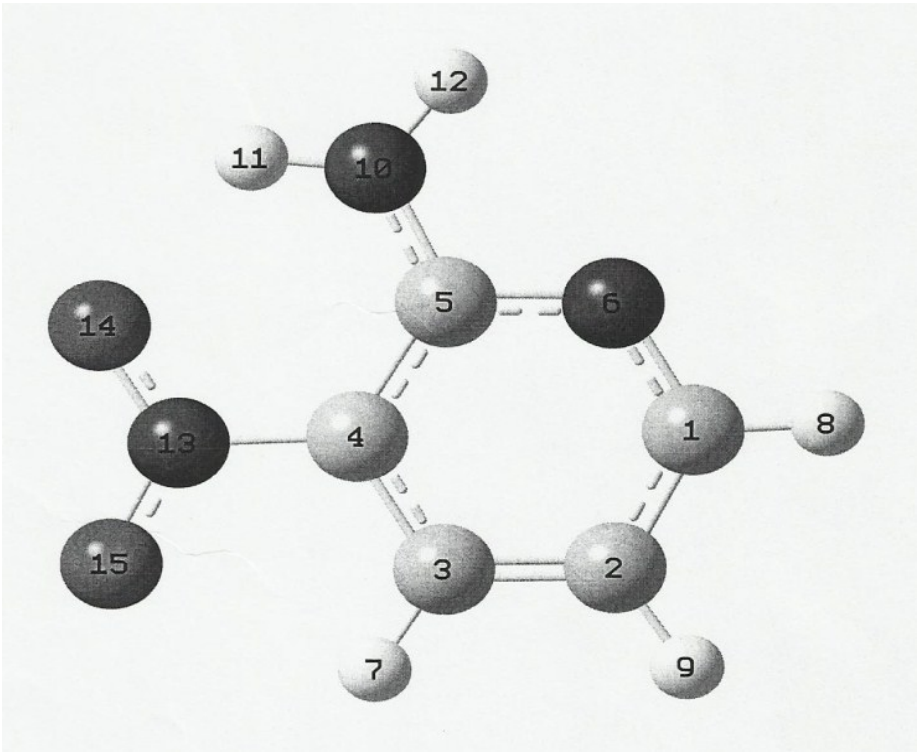

Figure 1. Optimized structure of ANP.

Table 1. Selected geometrical parameters optimized in ANP (bond length (Å), bond angle (°) and dihedral angle (°).

Parameters	MP2/6-311++G(d,p)	B3LYP/6-311++G(d,p)	Experimental XRD*
C_4-N_{13}	1.4651	1.4524	1.4382
N_{13}-O_{14}	1.2368	1.2386	1.2419
N_{13}-O_{15}	1.2300	1.2259	1.2902
C_5-N_{10}	1.3710	1.3467	1.3310
N_{10}-H_{12}	1.0091	1.0078	0.9186
N_{10}-H_{11}	1.0107	1.0072	0.9506
C_3-H_7	1.0848	1.0816	1.0409
C_2-H_9	1.0844	1.0817	0.9530
O_{14}-N_{13}-O_{15}	124.5381	118.3157	121.8500
C_5-C_4-N_{13}	121.9160	118.4668	121.9700
N_6-C_5-N_{10}	115.8050	115.5705	115.2700
H_{12}-N_{10}-H_{11}	117.1086	122.5689	109.1300
N_6-C_1-H_9	115.4116	115.5705	116.3500
$O_{14}N_{13}$-C_4 C_5	-24.3622	-0.0123	4.0600
$O_{14}N_{13}C_4$ C_3	154.7733	-0.0081	-175.6600
$H_{12}N_{10}C_5N_6$	-14.6684	180.0414	-0.0195
$H_{11}N_{10}C_5N_6$	-155.5782	-0.0195	179.5900
*Data taken from Ref. 8.			

Natural Population Analysis

Table 2 listed the natural atomic charges of the title compound together with Mulliken charges calculated by B3LYP/6-311++G(d, p) level of theory and basis set. The results showed redistribution of electron density among the atoms due to the hydrogen bonding interaction. The N_{10} acquires highly negative charge compared with the other N atoms in the compound and the H_{12} and H_{13} hydrogen atoms become more acidic.

Table 2. Natural atomic charges (e) of ANP calculated at B3LYP/6-31++G(d, p) level of the theory and basis set.

Atom	NBO charges	Mulliken atomic charges
C_1	0.116	-0.316
C_2	-0.292	-0.173
C_3	-0.125	0.170
C_4	-0.012	-0.088
C_5	0.419	-0.083
N_6	-0.488	-0.145
N_{13}	0.443	-0.229
N_{10}	-0.783	-0.323
O_{14}	-0.374	-0.058
O_{15}	-0.420	-0.021
H_7	0.245	0.268
H_8	0.191	0.197
H_9	0.222	0.185
H_{13}	0.428	0.316
H_{12}	0.401	0.301

Vibrational Assignments

The IR spectrum of the investigated molecule was recorded as KBr disc in the range 4000 – 400 cm^{-1} (see Figure 2). The detailed vibrational assignment of fundamental modes of 2-amino-3-nitropyridine along with calculated IR wavenumbers at B3LYP and MP2 level using 6-311++G(d, p) basis sets have been collected in Table 3.

According to the theoretical calculations, 2-amino-3-nitropyridine (ANP) has structure of C_s point group. The molecule has 15 atoms and 39 normal modes of vibrations. All the fundamental vibrations are active in both IR and Raman. The normal vibrations are distributed as 27 A' (in plane) and 12 A" (out-of plane) coordinates.

The results showed that the DFT (B3LYP) and MP2 methods applied in this work leads to vibrational wavenumbers which are in good agreements with the experimental data. The small difference between the experimental and calculated vibrational modes could be attributed to the formation of intermolecular hydrogen bonding and to the fact that the experimental results belong to solid phase while the theoretical belong to isolated gaseous phase.

C-NH_2 Vibrations

The $–NH_2$ symmetric and asymmetric stretches in the range of 3717-3575 cm^{-1} are in agreement with experimental value in the range of 3630-3488 cm^{-1}. The calculated $–NH_2$ scissoring vibration at 1656 cm^{-1} is in excellent agreement consistent with the expected characteristic value at 1593 cm^{-1}. The NH_2 rocking mode has been identified at 1095 cm^{-1} and also in agreement with the computed value at 980 cm^{-1}. The NH_2 wagging computed at 425 cm^{-1} show excellent agreement with FT-IR experimental data at 410 cm^{-1}.

-NO_2 Vibrations

The characteristic group wavenumbers of the nitro group are relatively independent of the rest of the molecule, which make this group convenient for identifications. Aromatic nitro compounds have strong absorption due to the asymmetric and symmetric stretching vibrations of the NO_2 group at 1647 and 1595 cm^{-1} respectively. The hydrogen bonding has little effects on the NO_2 asymmetric vibrations.[15] In the present investigation, values of asymmetric and symmetric modes of vibrations are computed at 1656 and 1378 cm^{-1} respectively in agreement with the experimentally recorded values at 1593 cm^{-1} and 1310 cm^{-1}. The bending vibrations of NO_2 group (scissoring, rocking, wagging and twisting) contributed to several normal modes in the low frequency region. It flows from Table 3 that the bands computed at 843 cm^{-1} and 716 cm^{-1} are assignable to NO_2 scissoring and wagging respectively in good agreement with the corresponding experimental data.

C–H Vibrations

The heteroaromatic structure shows the presence of C–H stretching vibrations in the range of 3100–3000 cm^{-1} [15] which is the characteristic region for the ready identification of C–H stretching vibrations, and the bands are not affected by the nature of substitutents. Hence the band at 3100 cm^{-1} has been designated to C–H stretching in agreement with the theoretically calculated value at 3221 cm^{-1}. The computed out of plane bending vibration of C – H at 992 cm^{-1} is comparable with the experimentally observed value at 950 cm^{-1}.

C–H---O hydrogen Bonding

In addition to the strong intramolecular hydrogen bond, H_{11}---O_{14}, DFT predicts the weak hydrogen bonding interaction H_7---O_{15}. Recently it has been established that a C–H group can be a hydrogen bond order. Although the C–H---O interactions are considered weak they form 20-25% of the total number of hydrogen bonds constituting the second most important

group.[16] This interaction could be of greater importance in NLO-systems. *Ab-initio* calculations have been particularly useful in the identification of C–H---O hydrogen bonds in which the C–H donor group is strengthened, shortened and blue-shifted (U-shifted in the stretching vibrational wavenumber.[17] The intramolecular contacts of H_7---O_{15} occurs with H---O distance of 2.67Å which is significantly shorter than the Van der Waals separation between the oxygen atom and the H-atom (2.72 Å) indicating the possibility of the intramolecular C–H---O interaction in 2-amino-3-nitropyridine. The calculated C–H---O angle for this interaction is well within the angle limit as the interaction path is not necessarily linear.[18]

Table 3. Experimental and B3LYP level computed vibrational frequencies (cm^{-1}) obtained for 2-amino-3-nitropyridine.

Experimental wave number (cm^{-1})	B3LYP/ 6-311++G(d,p) theoretical wave number (cm^{-1})			PM2/ 6-311++G(d,p) theoretical wave number(cm^{-1})			species	Assignment
	unscaled	scaled	IR-Intensity kCal/mol	unscaled	scaled	IR-Intensity kCal/mol		
3630	3717	3394	105	3727	3511	108	A\	$\nu_a(NH_2)$
3488	3575	3264	88	3578	3370	87	A\	$\nu_s(NH_2)$
3100	3221	2941	4	3230	3043	5	A\	ν(CH)
3085	3204	2925	3	3210	3024	3	A\	ν(CH)
3055	3151	2877	17	3171	2987	18	A\	ν(CH)
1593	1656	1512	506	1662	1566	530	A\	ν(ring)+ν(CN)+δ(CH)+ $\delta(NH_2)$ + $\nu_{as}(NO_2)$
1542	1610	1470	109	1620	1526	110	A\	ν(ring)+δ(CH)+δ(NH_2)+ $\nu_{as}(NO_2)$
1535	1595	1456	81	1610	1517	83	A\	$\nu_{as}(NO_2)$+$\delta(NH_2)$+ ν(ring) + δ(CH)
1530	1553	1418	158	1562	1471	157	A\	ν(ring)+$\nu_{as}(NO_2$-)+δ(NH) + δ(CH)
1465	1477	1349	43	1470	1385	41	A\	δ(CH) + δ(NH)+ν(ring)

1415	1470	1342	104	1473	1388	104	A′	$\delta(NH_2)+\delta(CH)+\nu(ring)+ \nu_s(NO_2)$
1310	1378	1258	49	1385	1305	51	A′	$\delta(CH)+\nu(CN)+\delta(NH_2)+ \nu_s(NO_2)$
	1357	1239	143	1310	1234	17	A′	$\delta CH+\delta NO_2+\nu CN+$ vring
1210	1298	1185	16	1295	1220	16	A′	$\delta(CH)+\delta(CN)+\nu(NO_2)+ \nu(ring)$
	1284	1172	338	1283	1209	340	A′	$\nu(ring)+\delta(CH)+\delta(CN)+ \nu(NH) + \nu(CN)$
1120	1172	1070	9	1182	1113	9	A′	$\delta(CH) +\nu(CN) + \nu(NO)$
1055	1105	1009	48	1103	1039	48	A′	$\delta(CH)+\nu(CN)+\delta(ring)+ \rho(NH_2)$
980	1095	1000	10	1092	1029	10	A′	$\delta(CH)+ \nu(CN) + \rho(NH_2)$
930	1008	920	1.5	1009	950	2	A′	$\delta(CH)+\nu(ring)+\rho(NH_2) + \nu(NO)$
950	992	906	≈1	987	930	≃ 1	A″	bend (op)CH
948	990	904	≈1	988	931	≃ 1	A″	bend (op)CH
870	915	835	17.5	910	857	18	A′	$\delta(ring)+\delta(NO_2)+ \nu(CN)$
790	843	770	15	841	792	15	A′	$\delta(NO_2)+ \nu(ring) + \nu(CN)$
733	795	726	31.5	792	746	32	A″	bend (op) CH
	750	685	11	755	711	11	A″	bend (op) CN+bend (op) ring + bend (op) CH
680	716	654	13	715	674	13	A″	bend (op) ring+bend (op) CH + $\omega (NO_2)$
610	678	619	4	677	638	4	A′	$\delta(ring) + \delta(NO_2)$
592	642	586	7	640	603	7	A″	$t(NH_2)$
610	581	530	≈ 2	583	549	≃ 2	A′	$\delta(ring) + \nu(CN)$
492	545	498	8	543	512	8	A′	$\rho(NO_2)+\rho(NH_2)+\rho(ring)$
	540	493	8	540	509	8	A″	bend(op) ring +bend (op) CH
	425	388	16	525	495	16	A″	bend (op) CH+

								bend (op) ring + ω NH_2
	405	370	5	403	380	5	$A^{\prime}$	ρ(NO_2) + ρ(NH_2) + bend (ip) ring
	389	355	4	388	365	4	$A^{\prime\prime}$	ρ (NH_2) + bend (op) ring
	321	293	200	325	306	200	$A^{\prime}$	ρ (NH_2)
	288	263	5	281	265	5	$A^{\prime}$	ρ (NO_2)
	234	214	1.8	233	219	1.8	$A^{\prime\prime}$	bend (op) ring
	117	107	~ 0	116	109	~ 0	$A^{\prime\prime}$	bend (op) ring
	67	61	1.5	67	63	1.5	$A^{\prime\prime}$	t(NO_2) + bend (op) ring
δ: scissoring; ρ: rocking; ω: wagging; t: torsion; ν_s: symmetric stretching; ν_{as}: asymmetric stretching; ip: in-plane bending; op: out-of-plane bending.								

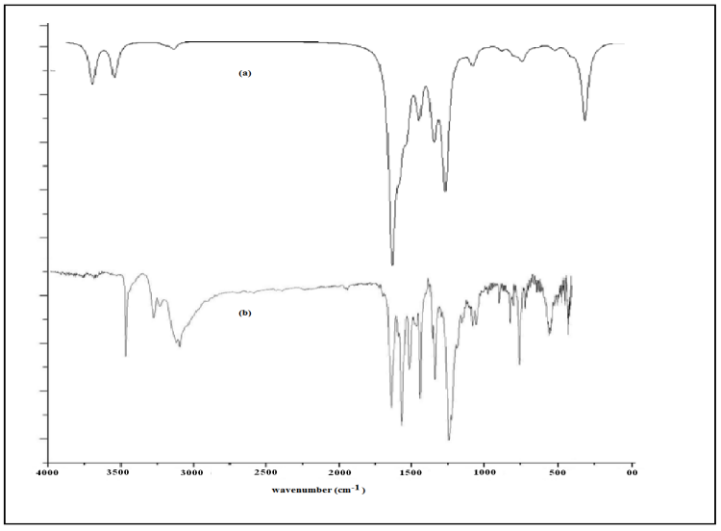

Figure 2. FT-IR spectrum of ANP (a) computed with B3LYP/6-31++G(d, p) (b) experimental.

Natural Bond Orbital Analysis

Natural bond orbital (NBO) analysis provides an efficient method for studying intra- and intermolecular bonding and charge transfer or conjugated interaction in molecular systems.[19] NBO analysis has been performed on the investigated compound to identify and explain the formation of intramolecular hydrogen bonding between C-H of pyridine ring and oxygen atom of nitro group in the molecule and delocalization of energy difference (ED) within the molecule.

Table 4. Second–order perturbation theory analysis of Fock-matrix in NBO analysis corresponding to the intermolecular C-H--O hydrogen bonds of ANP.

Donor NBO(j)	Acceptor NBO(d)	$E^{(2)}$ KJ/mol[a]	E(j)-E(i) a.u[b]	F(i,j) a.u[c]
LP_2O_{15}	$\sigma^* C_3$-H_7	0.65	0.76	0.02
LP_2O_{14}	$\pi^* N_{10}$-H_{11}	6.46	0.79	0.065

[a]$E^{(2)}$ means energy of hyperconjugative interactions (stabilization energy).
[b]Energy difference between donor and acceptor i and j NBO orbitals.
[c]F(i,j) is the Fock matrix element between i and j NBO orbitals.

The intramolecular C–H---O hydrogen bonds are exposed in Table 4 by the interaction between the oxygen lone-pairs LP_2O_{15} and the antibonding $\sigma^* C_3$-H_7 not withstanding that the energetic contribution (0.65) of hyperconjugative interaction are weak, these $E^{(2)}$ values are chemically significant and can be used as a measure of the intramolecular delocalization. The strengthening and contraction of C_3-H_7 bond is due to rehyperdization[20], which is revealed by the low value of ED (0.76) in the σ^* C_3–H_7 orbitals.

NMR Spectra

The molecular structure of the title compound was optimized, then, gauge-including orbital (GIMO) ^{13}C-NMR and ^{1}H-NMR chemical shifts calculations of the title compound were carried out using B3LYP/6-31++G(d, p) method. The calculations were performed in DMSO solution using IEF-PCM model, rather than in the gas phase and the values obtained were compared with experimental data and the data are listed in Table 5. The results showed excellent agreement between experimental and computed chemicals shifts. Figures (3&4) show experimental NMR spectra of ANP.

Table 5. ^{1}H and ^{13}C-NMR chemical shifts (δ, ppm) for 2-amino-3-nitropyridine (ANP).

Chemical shift ppm	^{1}H					^{13}C				
	H_{13}	H_9	H_{12}	H_8	H_7	C_1	C_2	C_3	C_4	C_5
Experimental	6.8	7.3	8.8	9.0	9.2	145	100	125	120	140
Computed	6.5	7.2	8.3	8.7	8.9	143	98	123	117	138

Electronic Properties and UV Spectra

The UV-Vis absorption spectrum of the sample in ethanol is shown in Figure (5) together with the experimental spectrum in the same solvent. On the basic fully optimized ground-state structure, TD-DFT/B3LYP/6-311++G(d,p) calculations have been used to determine the low-lying excited states of ANP. The calculated results involve vertical excitation energies, oscillator strength (*f*) and wavelengths. Typically according to Frank-Condon principle, the maximum absorption peak (λ_{max}) corresponds in an UV-Vis spectrum to vertical excitation. TD-DFT/B3LYP/6-311++G(d,p) predicts one intense electronic transition at (260.85 nm) with an oscillator strength *f*=0.3685, that shows excellent agreement with measured experimental data (λ_{max}=260 nm) as shown in Table 6.

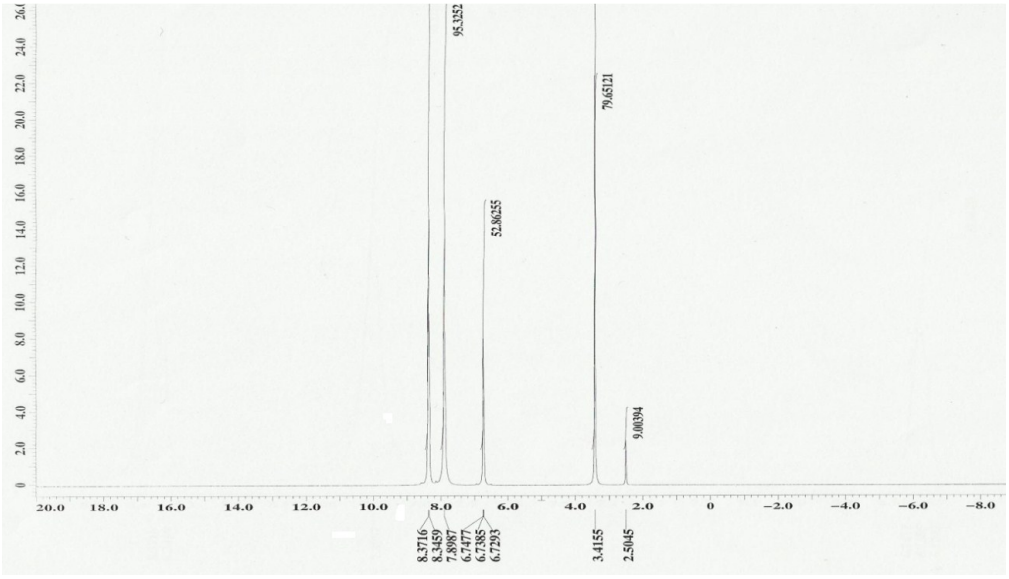

Figure 3. Experimental ^{1}H-NMR of ANP.

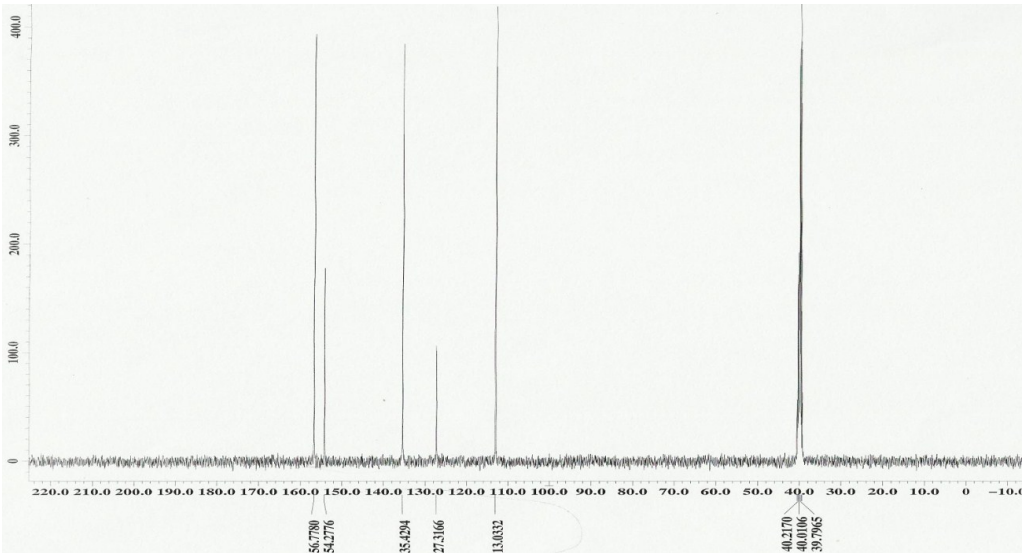

Figure 4. Experimental ^{13}C-NMR of ANP.

Both the highest occupied molecular orbital (HOMO) and lowest unoccupied molecular orbital (LUMO) are the main orbitals taking part in chemical reactions. The HOMO energy characterizes the ability of electron donating; LUMO characterizes the ability of electron accepting. The energy gap between the highest occupied and the lowest unoccupied molecular oribtals characterizes the molecular electrical transport properties because it is a measure of electron conductivity. The energy gap is largely responsible for the chemical and

spectroscopic properties of the molecules.[21] This also used by the frontier electron density for predicting the most reactive position in π- electron systems and also explains several types of reactions in conjugated systems.[22]

The HOMO is located over the NO_2 and NH_2 groups, the HOMO-LUMO transition implies an electron density transfer to pyridine ring from N=O and N-H bonds. The HOMO and LUMO orbitals significantly overlap in the position for ANP. The molecular orbitals are sketched in Figure (6).

The calculated self-consistent field (SCF) energy of ANP is (−508.189 a.u). The HOMO-LUMO energy gap explains the eventual charge transfer interactions taking place within the molecule. The small value of band gap reflects the chemical activity of the molecule and encourages the application of ANP as non-linear optical materials.

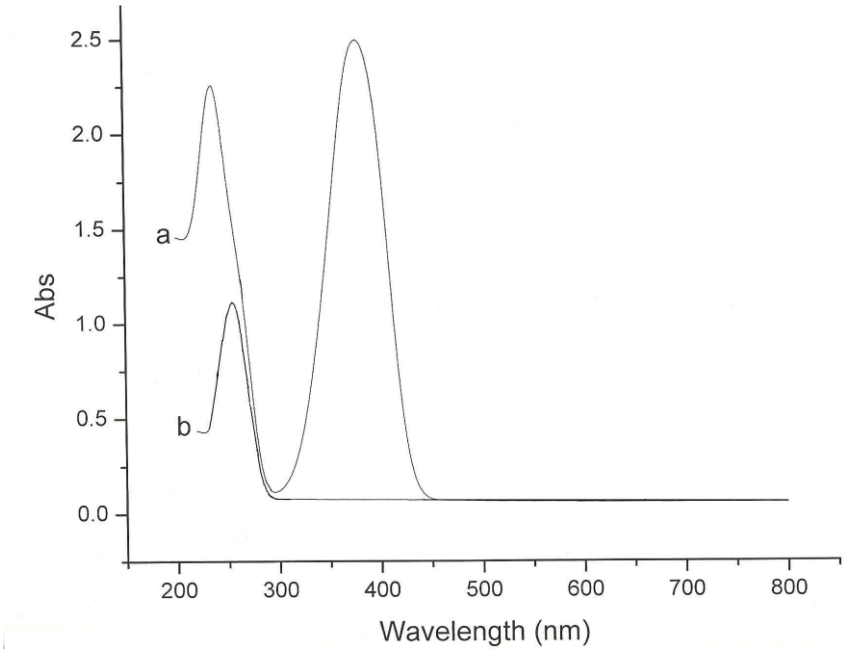

Figure 5. The Experimental UV-vis of ANP (a) and theoretical (b).

Table 6. The UV-vis excitation energy (ΔE) and oscillator strength (*f*) for ANP calculated by TD-DFT/ B3LYP/6-31++G(d,p) method.

λ_{obs}(nm)	B3LYP/6-31++G(d,p) λ_{Calc}(nm),		Excitation energy (eV)	*f*
380	--		--	---
260	260.85	$\sigma \rightarrow \sigma^*$	4.7531	0.3685
---	238.57	$\pi \rightarrow \sigma^*$	5.6966	0.002
---	220.95	$n \rightarrow \sigma^*$	6.0490	0.0129

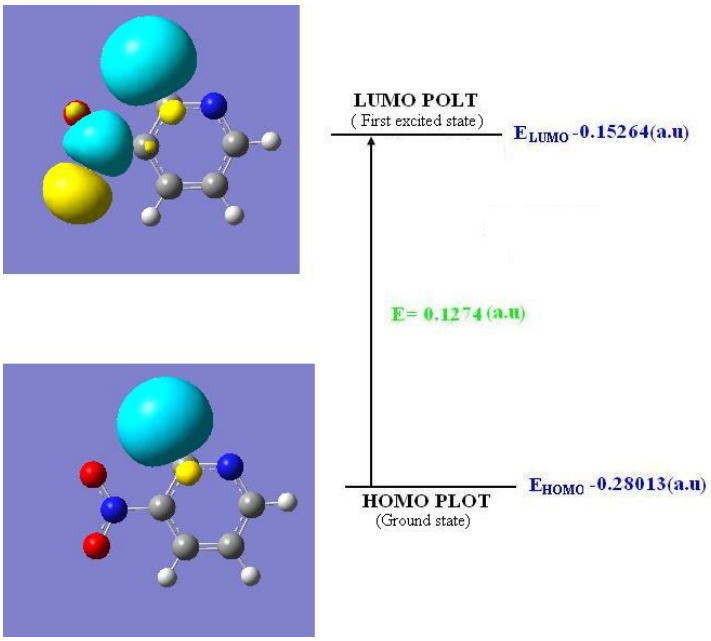

Figure 6. HOMO and LUMO orbitals and energy plot of ANP.

Thermodynamic Properties

Several calculated thermodynamic parameters are presented in Table 7.

Table 7. Theoretically calculated energies (a.u), zero point vibration energies (Kcal mol^{-1}), rotational constants (GHz), entropy (Cal $mol^{-1}K^{-1}$) and dipole moment (D) for ANP.

Parameters	B3LYP/6-311G++(d,p)
Total energy (electronic + zero point energy)	−508.081863
(electronic + thermal energy)	−508.073915
Zero point energy	67.85
Rotational constants	2.3764 1.2825 0.8329
Entropy	
Total	88.225
Translational	40.700
Rotational	29.228
Vibration	18.297
Dipole moment(vacuum)	3.4719

Dipole Moment

Asymmetric molecules generally have non-zero dipole moments in the respective ground electronic states. Based on the stable geometry of ANP in the ground state, the dipole moment in vacuum and in different solvent environments was calculated using TD-DFT. The dipole moment is found to increase with an increase in solvent polarity and this facilitates the charge transfer probability. The high values of dipole moment of ANP signifies high delocalization of charges, resulting in the formation of relatively loose structured, charge separated species.

Conclusion

Geometric optimization, FT-IR, NMR and UV-Vis spectra have been computed by DFT using B3LYP/6-311G++(d,p) level of theory and basis set combination.

The results showed good agreement between the experimental and theoretical data indicating the validity of the DFT level of theory and basis applied to ANP molecule for prediction of both structural and spectroscopic data of the title compound. The investigation of C-H···O intramolecular interaction in 2-amino-3-nitro pyridine by DFT showed that the calculated C-H···O angle for this interaction is well within the angle limit as the interaction is not necessary linear. The small HOMO-LUMO energy gap value computed using DFT indicates that the title compound could be of potential use as non-linear optical material (NLO).

Acknowledgment

The Authors extend their appreciation to the Deanship of Scientific Research at King Saud University for funding the work through the research group project NO RGP-VPP-041.

References

1. Bernstein J and Hagler A T, *Cryst. Liq. Cryst.,* 1979, **50**, 223.
2. Threfall T L*, Analyst*., 1995, **120,** 2435.
3. Pecaut J, Levy J P and Masse R, *J. Mater. Chem.*,1993*,* **3**, 999.
4. Nicoud J F, Masse R, Bourgogne C and Evans C, *J. Mater. Chem.*, 1997, **7**, 35.
5. Masse R, Bagieu-Beucher M, Pecaut J, Levy J P and Zyss J, *Nonlinear optics*, 1993, **5**, 413.
6. Okamato M, Takahashi K, Doi T and Takimoto Y, *Anal. Chem.*, 1997, **69**, 29.
7. Szafran Z D, Kania A, Wyadra B N and Szafran M, *J. Mol. Struct.*, 1994, **322**, 223.
8. Aakeroey C B, Beatty A M, Nievwenhuyzen M and Zou M, *J. Mat. Chem.*, 1988, **8**, 1385.
9. Jose S P and Mohan S, *Spectrochimica Acta A.*, 2006, **64**, 240. And references here in.
10. Sert Y, Ucun F and Böyükata M Z, *Natureforsch*, 2009**, 65a**, 107.
11. Gaussian Inc., *Gaussian 03 program*, Gaussian Inc., Wallingford, 2004.
12. Frish A, Nielsen A B and Holder A J, *Gauss View User Manual*, Gaussian Inc. Pittsburg, PA, 2001.
13. Kosmidis C, Bolovinos A and Tsekeris P, *J. Mol. Spect.*, 1986, **120**, 11.
14. Chocholousova J, Vladimir V S and Hobza P, *Phys. Chem. Chem. Phys*., 2004, **6**, 37
15. Bellamy L J, *The Infrared Spectra of Complex Molecules*, Wiley, New York, 1975.
16. Roeges N P G*, A Guide to the complete interpretation of infrared spectra of organic structures*, John Wiley & Sons, 1994

17. Weiss M S, *Trends Biochem. Sci*., 2001, **26**, 521.
18. Ribeiro-Claro P G A, Drew M G B and Félix V, *Chem. Phys. Lett*., 2002, **356**, 318.
19. Sato H, Dybal J, Murakami R, Noda I and Ozaki Y J, *J. Mol. Struct*., 2005, **744**, 35.
20. Hobza, P and Havlas Z, *Chem. Rev.*, 2000, **100**, 4253.
21. James C, Amal Raj A, Reghunathan R V, Jayakumar S and Habent Joe I, *J. Ram. Spect*., 2006, **37**, 1381.
22. Snehalatha M, Ravikumar C, Hubent Joe I and Jayakumar V S, *J. Ram. Spect*., 2009, **40**, 1121.